Journal Name

ARTICLE

Low cost and renewable sulfur-polymers by inverse vulcanisation, and their potential for mercury capture

D. J. Parker[a], H. A. Jones[a], S. Petcher[a], L. Cervini[c], J. M. Griffin[c], R. Akhtar[b], and T. Hasell*[a]

Received 00th January 20xx,
Accepted 00th January 20xx

DOI: 10.1039/x0xx00000x

www.rsc.org/

Sulfur is not only a highly abundant element, but also producd as a by-product of the petrochemicals industry. However, it has not been conventionally used to produce functional materials because polymeric sulfur is unstable, and decomposes back to its monomer. Recently, inverse vulcanisation has been used to produce stable polymeric materials with elemental sulfur as a major component. Here we report a series of alternative crosslinkers for inverse vulcanisation that are either low-cost industrial byproducts, or bio-derived renewables. These are shown to produce stable polymers with superior properties to previously reported materials. When made porous by the action of supercritical carbon dioxide or salt templating, these high sulfur polymers show excellent potential for mercury capture and filtration.

Introduction

There is a current global issue, arising from the petrochemicals industry, - the "excess sulfur problem".[1] Sulfur is a waste by-product of the purification of crude oil and gas reserves, where SO_2 is removed and converted, by hydrodesulfurisation, to S_8. This process produces ~70 million tons of elemental sulfur annually, and this figure is likely to increase as the global demand for energy forces the utilisation of more contaminated petroleum feed-stocks. While some of this sulfur is used for conversion to sulphuric acid or fertilisers, there remains an enormous unused supply. This is stored in megaton quantities and can be purchased for close to the cost of shipping. There has therefore been a recent interest in the possibility of forming this unwanted elemental sulfur into useful materials for commercial applications – it can effectively be seen as an inorganic equivalent to renewables. The most significant development in recent years has been the process of "inverse-vulcanisation".[1, 2] Elemental sulfur predominantly occurs as S_8 – a cyclic ring of 8 sulfur atoms. As a small molecule this has poor physical properties, and cannot be used as a functional material. However, when sulfur is heated above the floor temperature (159 °C) it is able to undergo ring opening polymerisation (Scheme 1a). Unfortunately, due to the reversibility of the S-S bonds this polymeric material is unstable, and readily depolymerises back to S_8. In the inverse-vulcanisation process an organic small molecule crosslinker (typically a diene) is added during sulfur-polymerisation (Scheme 1a). This acts to crosslink the sulfur chains and stabilise the material against de-polymerisation, creating a stable and functional material.

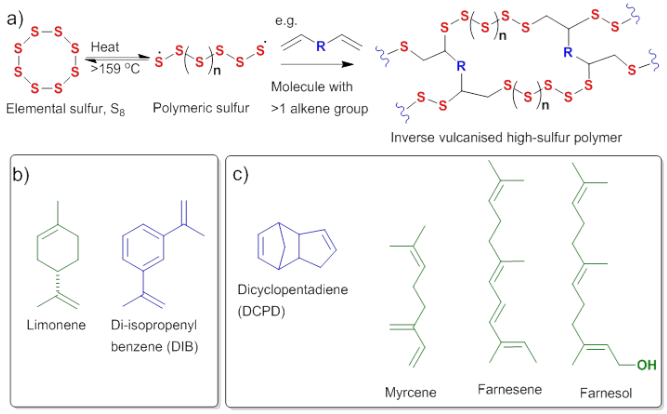

Scheme 1. a) Scheme of polymerisation of elemental sulfur and subsequent inverse-vulcanisation with an organic crosslinker. b) and c), structures of crosslinkers shown in green for renewable or blue for synthetic.

The high sulfur content (≥50 wt.%) in these materials gives them unique properties, and applications such as LiS batteries,[2-6] IR-transparent lenses,[7] and mercury capture.[8-10] Mercury is itself also an industrial by-product, and exists in the waste-streams of many industries. Mercury is of particular concern for human health because of its relative solubility in water and tendency to bioaccumulate and cause severe toxic effects.[11] Sulfur-polymers are therefore an attractive material for mercury filtration because sulfur is known as one of the most active sites for Hg adsorption.[12, 13] Two of the most significant inverse-vulcanised high-sulfur polymers reported to date have been sulfur-diisopropenyl benzene co-polymer (S-DIB),[2] and sulfur-limonene co-polymer (S-limonene)[8] (Scheme 1b). S-DIB is a shape persistent stable polymer, and perfectly suited for applications requiring a smaller amount of material, and making a high value product (e.g. batteries, lenses). However, the DIB crosslinker used to produce it is a relatively niche synthetic

[a] Department of Chemistry, University of Liverpool, Crown Street, Liverpool, L69 7ZD, UK email: T.Hasell@liverpool.ac.uk.
[b] Centre for Materials and Structures, School of Engineering, University of Liverpool, L69 3GH, UK.
[c] Department of Chemistry, Lancaster University, Lancaster LA1 4YB, U.K.
[Supplementary information available]. See DOI: 10.1039/x0xx00000x

chemical, and orders of magnitude more expensive than sulfur. This would be prohibitive in mercury capture applications. Mercury pollution of drinking water is a significant and global issue, especially in lower and middle income countries. Any material developed for Hg filtration has the potential to significantly improve health, and enable industrial development, but for widespread use a low cost of production will be crucial. Limonene therefore has a distinct advantage as a sulfur crosslinker, being a bio-derived renewable with low cost and large scale production (Scheme 1b). While this is far better suited to exploit the low cost of sulfur, the material produced has very poor physical properties and is not shape persistent – severely limiting its practical application. S-limonene forms more a hyperbranched polysulfide, of low molecular weight and glass transition temperature, than a true crosslinked polymer, and in physical appearance constitutes a thick viscous liquid rather than a solid.

Here we investigate a series of alternative crosslinkers (Scheme 1c) for the inverse vulcanisation of sulfur, and compare the properties of the resultant polymers with those of S-DIB and S-limonene. These polymers were chosen as potential crosslinkers that were either low cost bulk industrial feedstocks, in the case of dicyclopentadiene (DCPD), or bio-derived renewables, in the case of myrcene, farnesene, and farnesol. DCPD is readily available as it is coproduced in large quantities as a by-product in the steam cracking of naphtha and gas oils to ethylene. Myrcene, farnesene, and farnesol all occur naturally in many plants. The sulfur polymers produced show improved physical properties and successful mercury capture.

Experimental

Materials

1,3-disopropenyl benzene (DIB) was purchased from Tokyo Chemicals Industry. Sulfur, myrcene, farnesene, farnesol, and mercury chloride were purchased from Sigma-Aldrich. All chemicals were used as received.

Polymerisations

Polymerisations were carried out in open glass samples vials (12 or 40 mL volume) in aluminium heating blocks, with heating and stirring provided by electronic hotplates and magnetic stirrer bars. All reactions were begun by allowing the sulfur to fully melt, at 160 °C, before adding the organic crosslinker directly. Sulfur:crosslinker weight ratios were varied, but total mass was typically between 5 and 20 g. For DCPD, heating was maintained at 160 °C for 2 hours (the reaction vitrifies after typically ~20 minutes). Farnesene, farnesol, and myrcene reactions were all increased in temperature after the first 15 minutes, to 175 °C and maintained for a further 45 minutes. For all polymers, the colour becomes increasingly dark during the polymerisation, resulting in a black solid product. Moulded objects were prepared by polymerising the crosslinker and sulfur together as normal in a stirred glass vial, to ensure homogeneous mixing, before transferring them into a silicone mould and curing in an oven at 140 °C for 12 hours. The point to transfer the reaction mixture from the stirred vial to the mould was taken as the point at which an aliquot of the reaction mixture, when removed on a spatula and allowed to cool to room temperature, would no longer visibly separate to clear organic monomer, and precipitated yellow sulfur powder, but instead remain as a homogeneous brown viscous liquid.

Supercritical foaming

Substrate (~500 mg) was placed inside a glass vial in a stainless steel autoclave which was then filled with ~5.5 MPa of CO_2. The autoclave was then heated to 80 °C and topped up to 28 MPa. The $scCO_2$ was maintained under these conditions for 3 hours to allow the $scCO_2$ to infuse fully into the polymer, before rapid venting (less than one minute). Samples were granulated by breaking the solids up in a pestle and mortal before CO_2 treatment, and then again gently broken up afterwards to expose the internal surfaces.

Salt Porogen Synthesis

Sodium Chloride (90 g, 1.54 mol) was added to distilled water and stirred at 500 rpm for one hour to form a saturated solution. The solution was filtered under vacuum to remove remnant particulate salt. From the solution an aliquot (20 ml) was added to ethanol (200 ml). The resultant mixture was then filtered (Whitman filter paper) to a slurry which was then dried first under dynamic vacuum at room temperature, and then in an oven at 135 °C for half an hour.

Sulfur (2.5 g, 0.078 mol) was added to a sample vial, heated to 160 °C. DCPD (2.5 g, 0.019 mol) was added to the sample vial and stirred until one phase formed. The partially reacted liquid mixture was then poured into a mould and the salt porogen submerged into the liquid. After two minutes submerged the porogen was removed and placed into the oven at 135 °C for 24 hours.

Leaching: The resultant salt templated polymer was placed in boiling distilled water for 4 hours with stirring. Leached polymer was rinsed with distilled water and dried in an oven for 1 hour at 135 °C to remove water.

Characterisation

Scanning Electron Microscopy (SEM) imaging of the foamed polymer morphology was achieved using a Hitachi S-4800 cold Field Emission Scanning Electron Microscope (FE-SEM) operating in both scanning and transmission modes. The dry samples were prepared by dispersing the polymer powder directly onto adhesive carbon tabs. Imaging was conducted at a working distance of ~ 8 mm of 3 kV. Images were taken using a combination of both upper and lower detector signals.

The molecular weight of the soluble fraction of the polymers was determined by gel permeation chromatography (GPC) using a Viscotek system comprising a GPCmax (degasser, eluent and sample delivery system), and a TDA302 detector array, using chloroform as eluent, see ESI for full details.

Powder X-ray Diffraction (PXRD). Data was measured using a PANalytical X'Pert PRO diffractometer with Cu-$K_{\alpha 1+2}$ radiation, operating in transmission geometry.

Thermogravimetric Analysis (TGA). TGA was carried out in platinum pans using a Q5000IR analyzer (TA Instruments) with an automated vertical overhead thermobalance. The samples were heated at 5 °C/min to 900 °C under nitrogen.

Differential Scanning Calorimetry (DSC) were performed on a TA Instruments Q200 DSC, under nitrogen flow, and with heating and cooling rates of 5 °C/min.

Fourier-transform infrared spectroscopy (FT-IR) was performed using a Thermo NICOLET IR200, between 400 cm^{-1} to 4000 cm^{-1}. Samples were loaded either neat, using an attenuated total reflectance accessory, or in transmission after pressing into a KBr pellet.

Solution NMR was recorded in deuterated chloroform using a Bruker Advance DRX (400 MHz) spectrometer.

^{1}H and ^{13}C magic-angle spinning (MAS) NMR spectra were performed on a Bruker Avance III operating at a ^{1}H Larmor frequency of 700 MHz, using a Bruker 4mm HX probe. Chemical shifts were referenced using the CH_3 resonance of solid alanine at 1.1 ppm (^{1}H) and 20.5 ppm (^{13}C) (see ESI for full details). DFT calculations on polymer fragments: Computational calculations on the structural fragments were performed using Gaussian 09. Structures were generated using the GaussView package and fully optimized at the B3LYP level of theory using the 6-31G(d) basis set, before NMR parameters were calculated under the same conditions. For each polymer fragment shown in Scheme 2, cross-linking bonds were terminated with S-H groups prior to the calculations. A chemical shielding reference of 189.7 ppm was used, determined from a separate calculation on an optimized tetramethylsilane molecule.

Inductively coupled plasma optical emission spectrometry (ICP-OES) was performed at the Centre for Materials Science, University of Central Lancashire, on a Thermo Scientific iCAP 7400 ICP-OES. Results for each sample were run in triplicate and the average ppm recorded.

Hg capture: A stock solution of mercury was made by dissolving $HgCl_2$ in deionised water to a concentration of 2 ppm. 5 mL of this solution was placed in a series of glass sample vials along with 100 mg of sample. The sample vials were capped and stirred slowly by Teflon coated magnetic stirrer bars for 3 hours. The water was then decanted and filtered through a 0.25 µm nylon filter to remove any remaining solids, and analysed by ICP-OES.

Nanoindentation analysis

Nanoindentation was carried out using an Agilent nanoindenter G200 (Keysight Technologies, Chandler, AZ, USA) instrument with an XP indentation head. The indentations were performed at ambient temperature, aligned normal to the sample surface, using a Berkovich tip with a 20 nm radius. The samples were prepared by casting discs of the sulfur polymers in silicone moulds 3 cm wide and 5 mm deep. Conventional Oliver and Pharr analysis[14] was used to determine the elastic modulus and hardness. Each indent was made in the disc samples up to a maximum depth of 2000 nm with a 10s hold period at peak load. A Poisson's ratio of 0.35 was assumed in order to calculate the elastic modulus, chosen in comparison to glassy polymers poly(methyl methacrylate) and polystyrene.[15] 25 indentations were made on each sample as a 5 x 5 array with 50 µm spacing between each indent.

Results and discussion

Sulfur-DCPD co-polymer

DCPD is an ideal precursor for re-investigation in light of the current interest in inverse-vulcanisation; Reports from the 1970's describe the reaction of sulfur with DCPD, and suggest potential to form inverse-vulcanised materials.[16, 17] Sulfur-olefin reactions are characterized as low temperature reactions up to about 140 °C, and high temperature above 140 °C. High temperature reactions were thought to be complex, with both free-radical and cationic mechanisms and problematic reactions due to polymer degradation, poor reproducibility, and H_2S production – and therefore most of the chemistry carried out at this time was conducted at 140 °C and below.[1, 16] Reactions between sulfur and DCPD at 140 °C were found to produce soluble linear polymers, as reaction was limited to only one of the DCPD double bonds – that on the norbornene substituent (Scheme 2a). It was therefore aimed to investigate if S-DCPD reactions at higher temperatures could produce more highly crosslinked, inverse-vulcanised polymers – capable of producing functional materials – by careful control of reaction conditions.

There are many ways in which DCPD could be expected to react with sulfur (scheme 2). As well as reaction to form a linear polymer, as has been previously described,[16, 17] it was hypothesised that increased temperature would lead to a crosslinked structure by addition across the cyclopentene as well as norbornene double bond (scheme 2b). In addition to this, DCPD is known to crack to two molecules of cyclopentene on heating,[18] which could then react further with sulfur (scheme 2c). It is also possible to polymerise DCPD through ring opening metathesis polymerisation (ROMP). Normally metal catalysis is used,[19] although there has been recent interest in the development of metal free routes to polymeric DCPD.[20] Reaction occurs initially across the norbornene substituent to form a linear polymer which still contains a number of double bonds, but on continued heating crosslinking can occur through opening of the cyclopentene.[19, 21] Both the resulting linear polymer, and crosslinked material, contain double bonds and that could potentially further react with sulfur (scheme 2d and e). All of these mechanisms for reaction of DCPD with sulfur are possible, and it is likely the results are a combination of all to an extent, though the routes shown in scheme 2a and 2b would be expected to dominate.

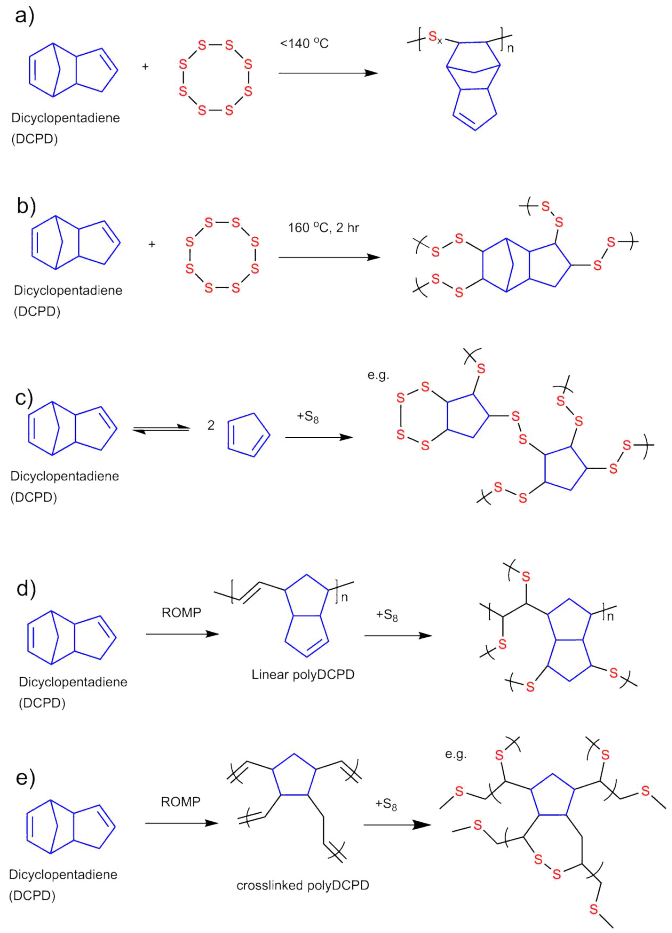

Scheme 2. Potential pathways for sulfur to react with DCPD: a) reaction of sulfur across the norbornene substituent only to form a linear polymer. b) inverse-vulcanisation across both double bonds to form a crosslinked material. c) cracking of DCPD to cyclopentadiene, followed by inverse vulcanisation of sulfur to produce a crosslinked polymer. d) Ring opening metathesis polymerisation of DCPD to form a linear polymer, followed by crosslinking with sulfur. e) Ring opening metathesis polymerisation to form a crosslinked polymer, and subsequent further reaction with sulfur.

Addition of DCPD to molten sulfur, at 160 °C, resulted in a clear pale yellow liquid, which becomes increasingly dark and viscous before vitrifying as a solid. Analysis of this material by TGA, in comparison to the starting materials, indicates a reaction has taken place (Fig. 1a). The resultant material is more thermally stable than either unreacted DCPD or sulfur, with a significant portion of mass remaining even after heating to 900 °C, indicating the formation of polymeric material. Further to this, the percentage mass remaining increases as a function of the proportion of DCPD used. FT-IR shows a reduction in the signals at 3047 and 1620 cm^{-1}, of the C=C-H and C=C stretching vibrations, as well as at ~700 cm^{-1} associated with cis di-substituted alkene C-H bend (Fig. 1b). It can also be noted that there is no signal detected at 2550-2620 cm^{-1}, which would be expected if thiol groups were present. This reduction, but not complete absence, of alkene positions would be consistent with a mostly crosslinked material, though with some linear polymer segments still present (i.e. a combination of scheme 2a, and 2b). Similarly, solution NMR of the initial stages of the reaction, before the products become insoluble, shows partial reaction at the C=C-H positions and the introduction of peaks in the δ ~ 3.5-4 ppm region corresponding to S-C-H protons (Figs. S1, S2.), consistent with reaction initially favouring mostly the cyclohexene position to produce a soluble linear product, before further reaction across the cyclopentene position renders the material insoluble.

Solid state NMR of the final insoluble material, after curing, shows similar results (Fig. 2). The ^{13}C cross-polarisation (CP)MAS spectrum (fig. 2a) shows there are certainly some double bond positions remaining (~135 ppm), and while the spectrum is not strictly quantitative, relatively low signal intensity was obtained for a range of CP contact times, indicating they are significantly less abundant that alkane carbons observed at ~30-60 ppm. The peak/shoulder in the 60-80 ppm region would be consistent with the presence of R-C-S, indicating significant sulfur crosslinking. The ^{1}H spectrum (Fig. 2b), gives consistent results, weak RC=C-H signal at ~4.5 ppm, strong broad signal for various alkane protons 0-3 ppm, and a shoulder consistent with S-C-H at ~3 ppm. The ^{1}H-^{13}C correlation spectrum (Fig. 2c) confirms the correlation of the positions assigned for S-C-H and C=C-H. DFT calculations were performed to simulate predicted spectra for the polymer fragments shown in Scheme 2, after structural optimization (Fig. S3). These models show greatest agreement with the experimental spectra for a combination of Scheme 2 a) and b) structures as the major phase. Minor components of the other proposed structures cannot be discounted fully though, and may well still be present, though only in small amounts.

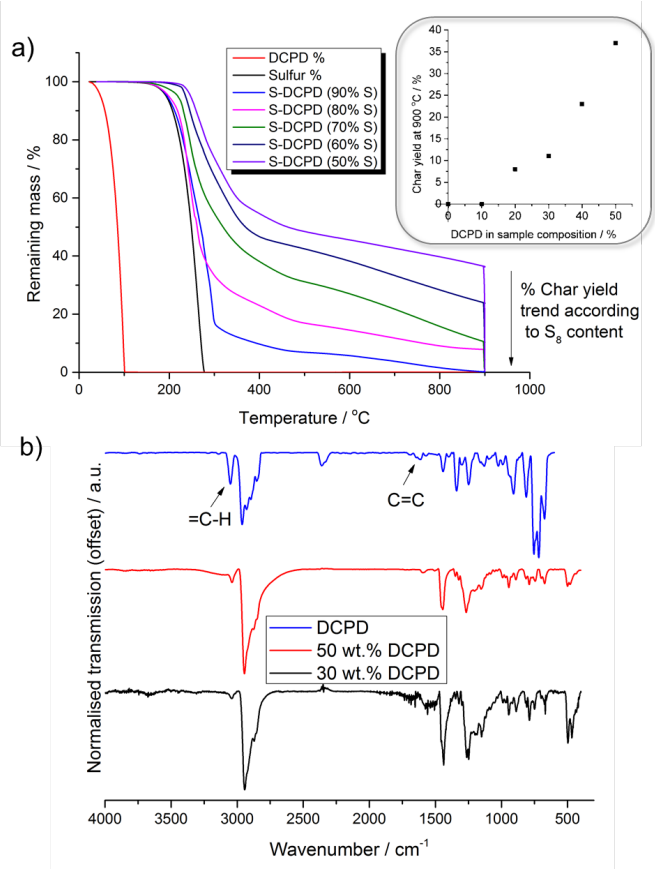

Figure 1. a) Thermogravimetric analysis of S_8, DCPD, and composite polymers. The % mass of char remaining at 900 °C, as a function of DCPD content, is shown in the inset. b) FT-IR spectra of DCPD (top), S:DCPD 50 wt%: 50 wt% (middle), and S:DCPD 70 wt%: 30 wt% (bottom).

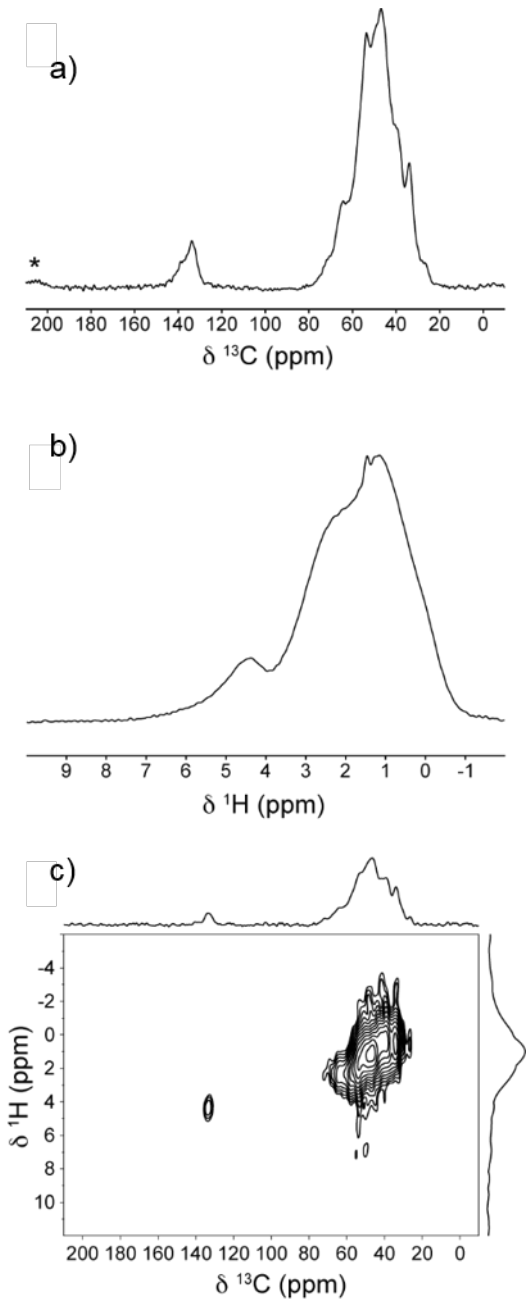

Figure 2. Solid state NMR spectra of a fully cured S-DCPD sample, (50 wt.% S): a) ^{1}H-NMR spectrum, b) ^{13}C-NMR spectrum, and c) ^{1}H-^{13}C heteronuclear correlation spectrum. The asterisk denotes a spinning side band.

Depending on the ratio of sulfur to DCPD, the initial colour of the samples varied from dark brown, for 90 wt% sulfur, through to black, for 50 wt% sulfur (Fig. 3a). Over 24 hours it could be seen that the 90 wt% sulfur sample became lighter brown in colour, and matt rather than glossy. This would be consistent with 'sulfur bloom', which is caused by the separation of elemental sulfur back out of the polymer, which crystallises as S_8, causing inhomogeneity. This was further confirmed by the detection of crystalline peaks corresponding to α-S_8 in the PXRD pattern of the 90 wt% sulfur sample (Fig. 3b), as well as the corresponding melting point in the DSC trace (fig. S4). This is consistent with similar results for S-DIB,[2] that found that only 10 wt% crosslinker was not sufficient to fully stabilise 90 wt% sulfur, and prevent depolymerisation. However, all of the other compositions at 20 wt% DCPD and higher showed no further change in appearance, or signs of S_8 separation by PXRD or DSC (Fig. 2b, S3), indicating that they are able to successfully stabilise the polymeric sulfur. The glass transition temperature, T_g, for the polymers was found to increase as a function of the DCPD composition (Fig. 2c), up to 115 °C for an equal mass composition of Sulfur and DCPD. This tendency of the T_g to increase with the amount of crosslinker used similarly observed for S-DIB, and presumably is caused by increased branching of the structure preventing chain movement. However, the highest observed T_g for S-DIB was 28 °C, and for S-limonene was -21 °C, all at the same 1:1 mass ratio. That S-DCPD exhibits a considerably higher T_g than S-DIB at similar compositions suggests more concerted crosslinking and increased stability in the structure. This higher degree of crosslinking is also supported by the complete lack solubility of S-DCPD in comparison to S-DIB or S-Limonene (Fig. 4). The relatively high solubility of S-limonene, being at least partially soluble in most solvents other than water, is a result of a its low molecular weight – described as a low molecular weight polysulfide rather than a high molecular weight polymer.[8] S-DIB has a lower solubility than S-limonene, and is only readily dissolved in certain organic solvents such as chloroform, tetrahydrofuran, and toluene. This is a result of a more extended polymeric structure, and higher molecular weight, in comparison to S-limonene. However, that S-DIB is soluble at all indicates that it forms what should be considered more as a highly hyper-branched, rather than fully crosslinked, polymer.[2]

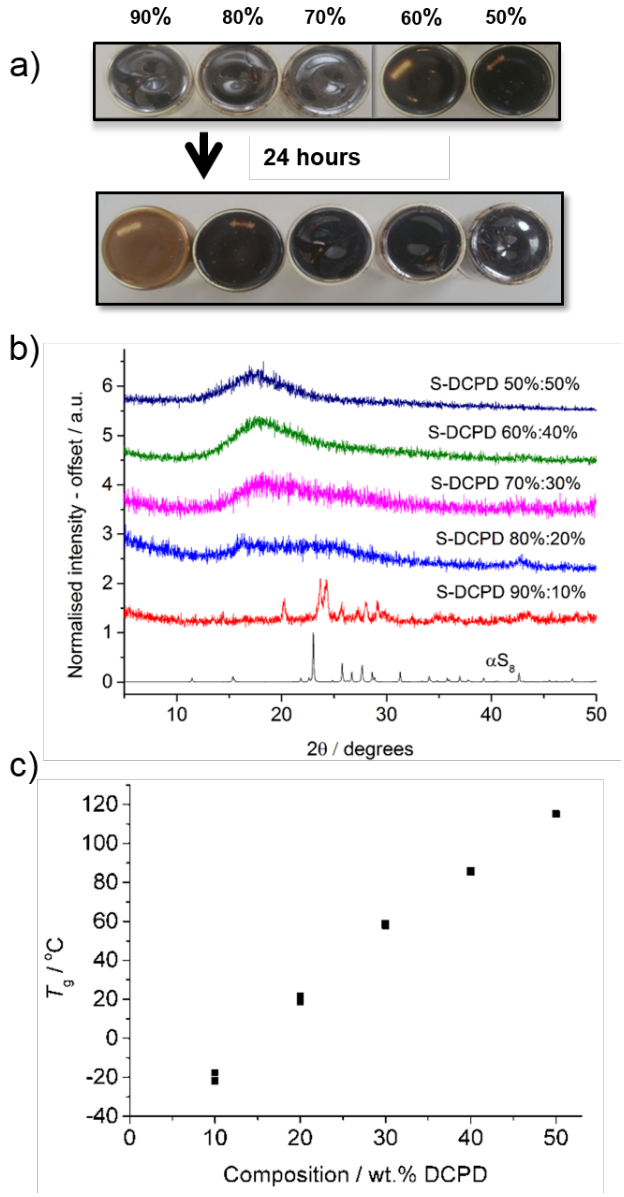

Figure 3. a) Photographic images of inverted vials of S-DCPD polymeric materials, synthesised at 160 °C for 2 hours, and their appearance after 24 hours. The percentage of sulfur by mass is indicated. b) The T_g of the S-DCPD polymers as a function of composition, showing two repeat measurements for each sample. c) PXRD patterns of S-DCPD and elemental sulfur. At 20 wt% DCPD and higher the materials are fully amorphous.

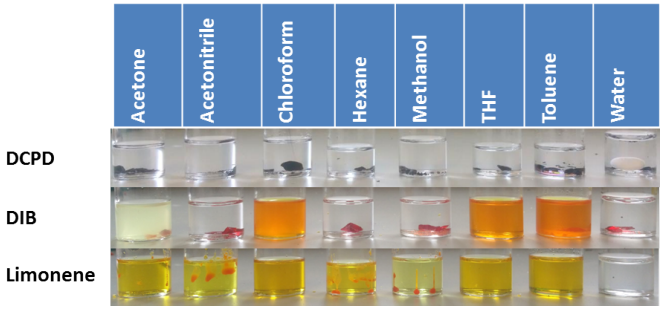

Figure 4. Photographic images demonstrating the solubility of aliquots of S-DCPD, S-DIB, and S-Limonene polymers (50 wt% sulfur) after stirring in solvent. S-DCPD remains insoluble in all of the solvents tested. Values in mg/mL in table S1.

During the course of performing reactions, it became apparent why previous studies may have largely avoided using >140 °C temperatures. The reactions occur in the absence of any conventional solvent, with both monomers (DCPD and sulfur) in a molten state, and were therefore found to be susceptible to the *Trommsdorff-Norrish* effect.[22] This effect is often found in neat monomer systems and is caused by an increase in viscosity during polymerisation leading to inhibition of the termination steps while initiation and propagation steps continue – leading to rapid auto-acceleration and often excessive exothermic reaction (Fig. 5). When this occurred it lead to a rapid expansion of the reaction mixture to form a solid foam. Further reaction would then stop due to the lack of mixing and poor heat transfer within the sample – leaving inhomogeneous products and incomplete reaction. However, with carful control of temperature it was found to be possible to prevent this, and even to produce a series of moulded objects (Fig. 6). The moulded objects were fabricated by first performing a pre-reaction in a glass vial at 160 °C with stirring for 2 hours, before transferring the reaction mixture to a silicone mould and curing in an oven at a lower temperature of 140 °C for a further 12 hours. This process is comparable to the reactive injection moulding used commercially for the fabrication of functional components from polymers that crosslink during synthesis, preventing post-synthetic processing. The agitated and higher temperature pre-reaction step is necessary to ensure sufficient reaction between the sulfur and the organic crosslinker that the mixture becomes homogeneous and does not phase separate in the curing step, and also to induce reaction across both double bonds. The longer but lower temperature curing step is necessary to ensure the reaction carries on to completion without triggering auto-acceleration and becoming excessively exothermic in the final stages. The end products are uniform, smooth, brittle solids with no detectible odour.

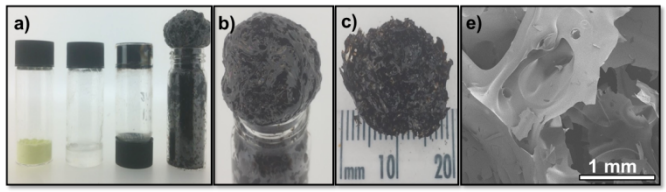

Figure 5. Images of reactants and products of a sulfur-DCPD reaction (50 wt% sulfur). a) Photographic images left to right, sulfur, DCPD, reaction products without foaming due to exothermic auto-acceleration (vial inverted), reaction products with exothermic auto-acceleration induced foaming. b) and c) Photographic images of foamed products. e) SEM image of large pores produced in foamed products.

Figure 6. Photographic images of various moulded objects produced from cured S-DCPD reactions, 5 pence coin and mm/cm graduations shown for scale.

Sulfur and renewable crosslinker co-polymers

Reaction of sulfur with each of the three renewable crosslinkers (myrcene, farnesene, and farnesol – scheme. 1b) yielded homogeneous black polymeric products (Fig. S5). All three co-polymers produced shape persistent solids (Fig. 7). However, S-farnesene co-polymer products were noticeably more malleable, followed by the myrcene, with farnesol producing the most physically rigid material. All three polymers show similar initial decomposition temperatures to S-DCPD, at over 200 °C (Fig. S5), though all had a lower proportion of char remaining by 900 °C than shown by S-DCPD. S-myrcene and S-farnesol both had significant char remaining by 900 °C, with the amount increasing with crosslinker content, but in the case of S-farnesene all mass was lost by 600 °C – consistent with the visual observation of a less stable/solid nature. Unlike S-DCPD, none of the 3 renewable sulfur co-polymers become fully insoluble (Fig. 8), indicating again that a hyperbranched structure is more likely, as for S-DIB and S-limonene. As the polymers showed solubility, gel permeation chromatography (GPC) was used to determine their relative molecular weight (Fig. 9). S-farnesene was found to have a low molecular weight, which may explain the relative malleability in comparison to the other polymers, and lower T_g (Fig. 10). S-myrcene and S-farnesol both contained a soluble and insoluble fraction in chloroform, and therefore the molecular weight cannot be taken as fully representative of the material, of which the less soluble fractions are likely to be of higher weight/ more crosslinked. The soluble fraction of S-myrcene was low molecular weight, though the soluble fraction of S-farnesol was higher, more comparable to that of S-DIB, likely explaining why S-farnesol shows the highest T_g of the three polymers (Fig. 10). PXRD, along with DSC, confirms that the incorporated sulfur is stable against decomposition back to S_8 at 50 wt% of crosslinker, though not below (Figs. S6, S7). FTIR and NMR confirm reaction of the double bonds of all three crosslinkers, and the formation of C-S bonds (Figs. S8-S13). The loss of the hydroxyl group suggests that the radical intermediates of farnesol are subject to etherification.[23] Terpenes such as farnesene and myrcene have been shown to polymerise under catalytic conditions,[24, 25] and therefore some homopolymerisation may be present in addition to crosslinking with sulfur.

Figure 7. Photographic images of moulded discs produced from cured S-farnesene, S-myrcene, and S-farnesol, from left to right respectively, with mm/cm graduations shown for scale.

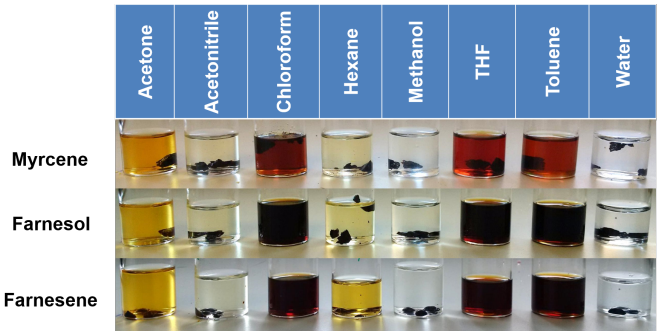

Figure 8. Photographic images demonstrating the solubility of aliquots of S-myrcene, S-farnesol, and S-farnesene polymers (50 wt% sulfur) after stirring in solvent. Values in mg/mL in table S1.

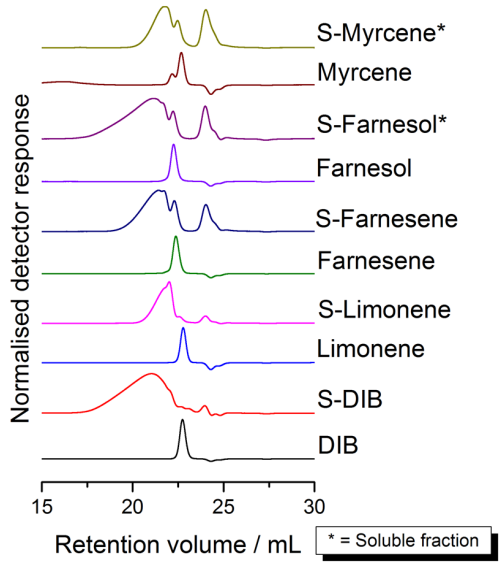

Polymer	M_w (g/mol)	M_n (g/mol)	PDI
S-DIB	8,450	882	9.58
	8,007	929	8.62
S-Limonene	904	493	1.83
	890	491	1.81
S-Farnesene	2,290	738	3.10
	2,298	745	3.08
S-Farnesol[*]	9,772	1,197	8.16
	10,118	1,195	8.47
S-Myrcene[*]	1,015	416	2.44
	962	401	2.40

Figure 9. GPC traces for sulfur-copolymers in chloroform, compared to a linear polystyrene standard. S-farnesol and S-myrcene were not fully soluble, and therefore the values are only representative of the fraction which was soluble. Molecular weights and polydispersity indices are shown in the table, with two repeat measurements for each.

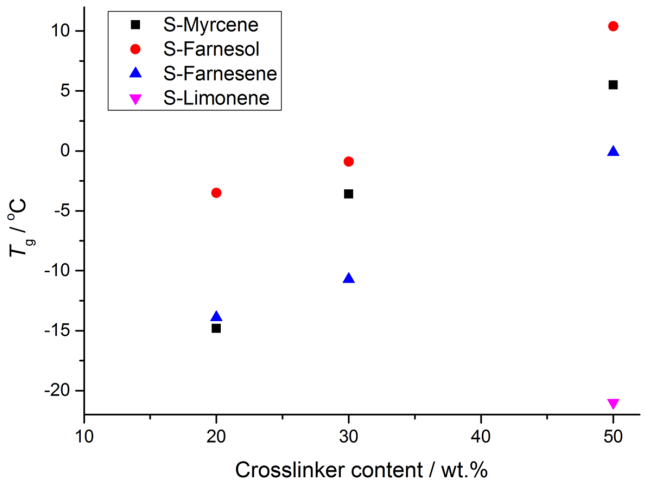

Figure 10. The glass transition (T_g) of sulfur-renewable crosslinker co-polymers as a function of crosslinker content.

Mechanical properties

For the polymers of sufficient rigidity, mechanical testing of their physical properties was performed. Nanoindentation was used to determine the displacement vs. load curves of the new co-polymers, in comparison to S-DIB (Fig. 11). The results allow the elastic modulus to be determined (Fig. 10), and indicate that S-DCPD is more ridged than S-DIB, presumably because of the more extensively crosslinked structure and considerably higher T_g. S-farnesol and S-myrcene, however, show lower rigidity, consistent with greater flexibility in the crosslinker molecules themselves w.r.t DIB and DCPD, and a less highly crosslinked structure with a lower T_g.

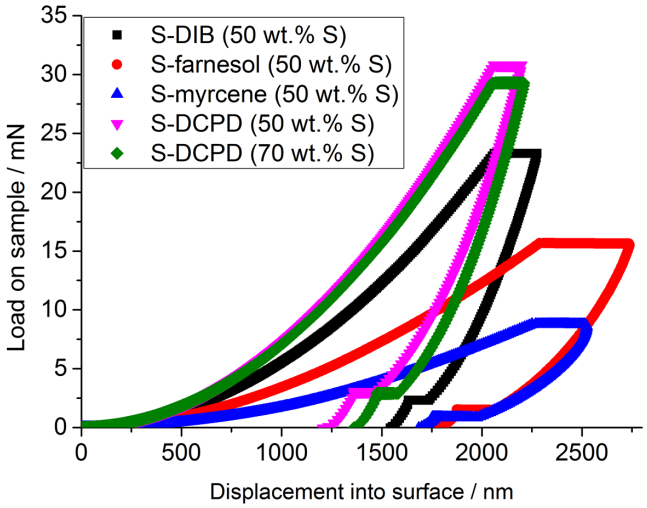

Figure 11. Load-displacement curves obtained via nanoindentation on discs of the sulfur co-polymers.

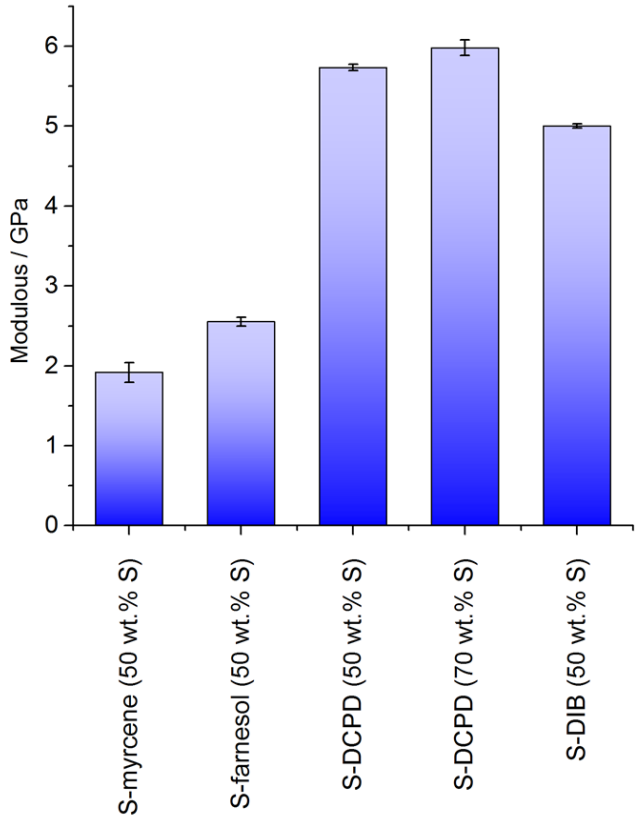

Figure 12. Elastic modulus results obtained from nanoindentation testing, showing the change in mechanical properties with composition. Standard deviation is shown as error bars.

Supercritical foaming, salt templating, and Hg capture

Samples of S-DCPD, S-myrcene, and S-Farnesol copolymers, all at 50 wt.% sulfur, were subject to foaming in supercritical CO_2, as had been previously demonstrated for S-DIB.[9] S-Farnesene was omitted from this study due to its lack of shape persistence. None of these three polymers foamed to the extent of S-DIB, which had a higher concentration of cells, and thinner cell walls.[9] It is likely that S-DIB foams well in $scCO_2$ because of a combination of its degree of crosslinking, molecular weight, and T_g. The hyperbranched rather than fully crosslinked structure, and just above room temperature T_g mean that it is easily swollen and plasticised by the CO_2, expanding to foam on CO_2 release, and then frozen in the expanded structure when cooled. S-DCPD still shows many internal voids created by the $scCO_2$ foaming, however, there is a thicker wall size and a noticeable jagged rather than smooth internal surface to the cavities (Fig. 13a). This roughness is likely caused by the more highly crosslinked structure being resistant to the expansion of the CO_2 to form bubbles upon pressure release. S-myrcene (Fig. 13b) showed no cell formation after the foaming step, but there was a roughening of the surface, possibly due to the physical action of the CO_2 venting, or the removal of low molecular weight material. The lack of foaming may be explained by the combination of crosslinking within the structure resisting cell formation and/or the relatively low T_g and physical softness of the material allowing cell collapse. S-farnesol however did show the formation of cell in the structure (Fig. 13c). The smooth surface of the cells, and large wall thickness/ low cell concentration would indicate a less crosslinked structure and partial collapse/relaxation of the cells after the venting step as a result of the lower T_g and more flexible structure in comparison to S-DCPD and S-DIB.

The supercritical foaming method of inducing porosity is inherently easier to perform post-synthetically, and as shown it may not be suitable for all types of S-polymer. Therefore an alternative route to generating porosity was sought. Salt templating provides a low cost and convenient alternative method, and is demonstrated here for S-DCPD. Micron-scale cubic NaCl crystals were first precipitated to a controlled size and allowed to fuse together (Fig. 14a). Partially-reacted liquid polymer was soaked into the salt template and cured to a solid polymer. The salt was then washed out leaving a connected network of pores throughout the polymer (Fig. 14b and 14c).

After foaming and salt templating, powder samples of the S-polymers were exposed to aqueous solutions of $HgCl_2$ to determine their ability for mercury capture. The S-DCPD, S-farnesol, and S-myrcene polymers, post foaming, all take up significant amounts of mercury (Fig. 15) – more than elemental sulfur or non-foamed samples of sulfur polymers S-DIB or S-limonene. While the powder particle size does affect the uptake, the foaming step is still clearly beneficial, with foamed samples of S-DCPD taking up more mercury than either coarsely or finely ground non-foamed samples, or the salt templated S-DCPD (Fig. S15). Of the foamed polymers, the Hg uptake will be a factor of both the available surface area, and the affinity of mercury for the exposed surface. It is therefore possible that although the foamed S-DCPD sample may have more available surface, the highly crosslinked stable structure may have less affinity for Hg in comparison to the hyperbranched S-farnesol and S-myrcene, which may contain more chain ends.

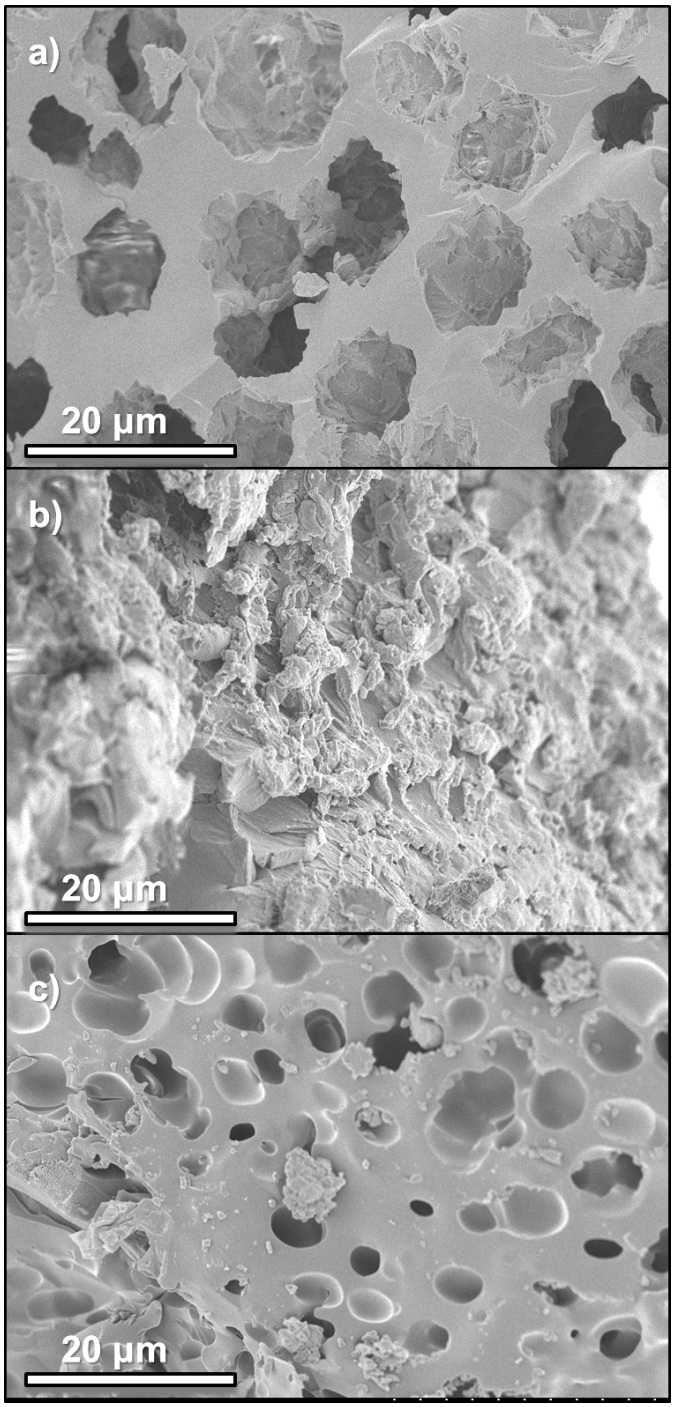

Figure 13. SEM imaging of $scCO_2$ foamed sulfur-copolymers (50 wt% sulfur): a) S-DCPD, b) S-myrcene, and b) S-farnesol. The sample shows both closed cell and connected macropores. Scale bars indicate 20 µm.

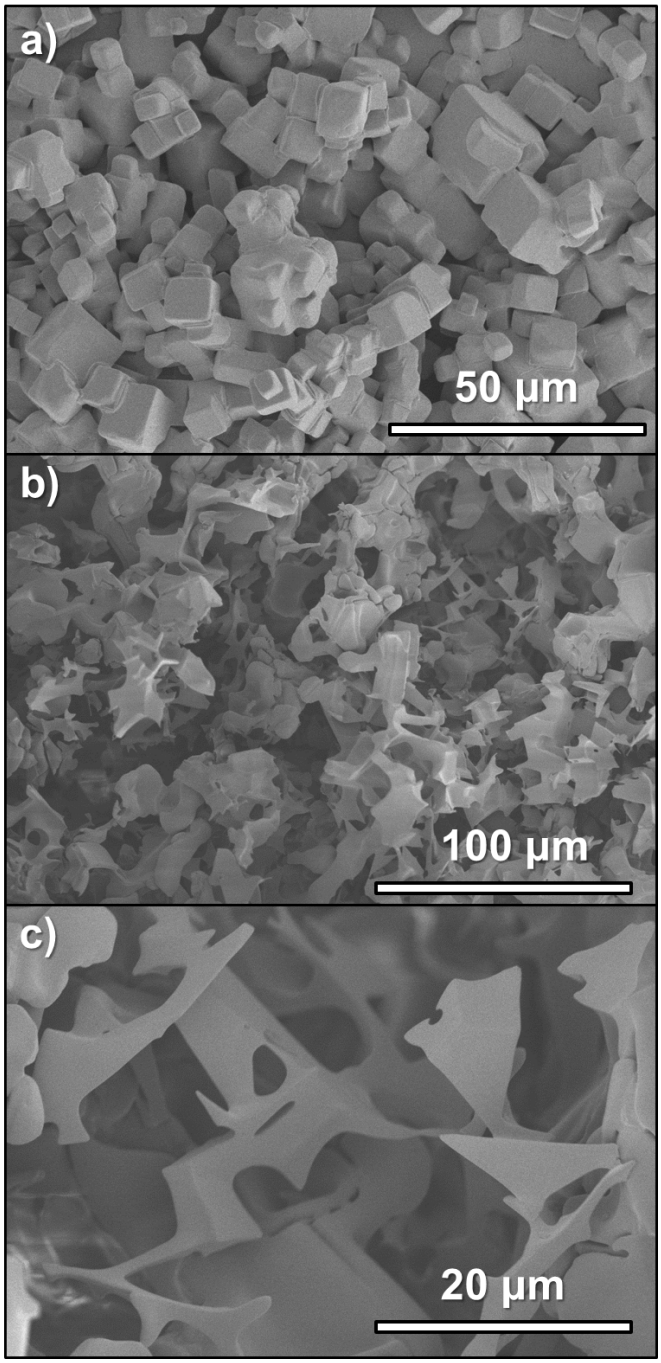

Figure 14. SEM imaging of salt templated sulfur-DCPD copolymers (50 wt% sulfur): a) The micro-precipitated and fused salt template, and b) and c) the S-DCPD after removal of the salt.

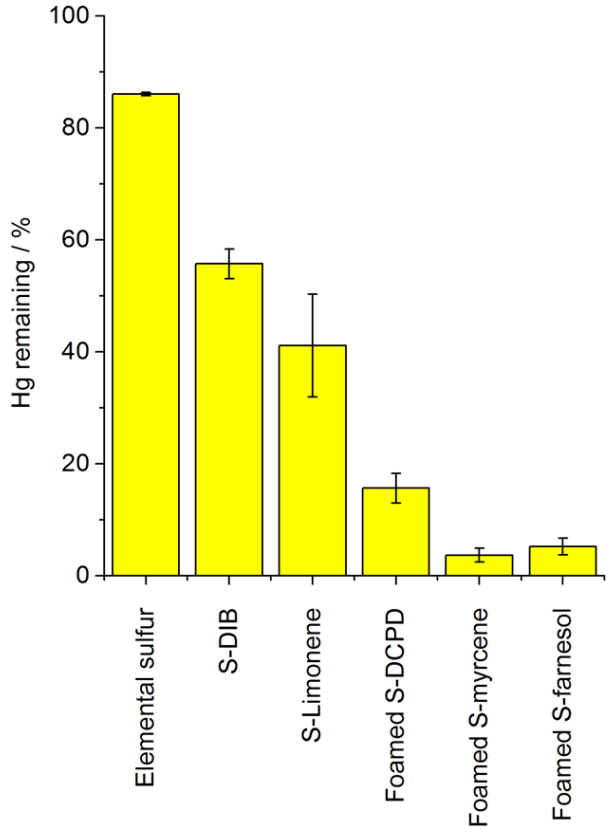

Figure 15. The percentage mercury remaining in solution after 3 hours exposure to each of the materials listed. Values are given as a mean of three repeats with standard deviation shown as error bars.

Conclusions

A range of inverse vulcanised compolymers with 50 wt% or higher of elemental sulfur have been synthesised. All of the polymers represent an excellent example of green chemistry: The monomers are comprised entirely of industrial by-products (sulfur and DCPD) and renewable organics (farnesene, myrcene, farnesol). The reaction is highly atom efficient, with no elimination. No solvents are required. The simplicity of the reactions and low cost of the reagents mean that these materials could be readily scaled up industrially. The low cost of the materials means they would be suitable in many conventional applications, especially where thermal or electrical insulation is important, and in the case of S-DCPD, also chemical resistance. The high stability of S-DCPD, in terms of its lack of solubility, and ability to prevent sulfur separating back out even at ratios of up to 80 wt% sulfur, can both be attributed to an intimately mixed and highly crosslinked structure. In terms of advanced applications, high sulfur polymers have already been demonstrated for electrical[2-5] and optical[1, 7] applications. One important application of sulfur-polymers is Hg capture, and the new materials reported here show great potential for Hg capture as there is considerable scope to increase porosity and the amount of available surface area further. The scale at which materials would need to be produced for practical application in Hg capture, and the necessity for commercial viability, make these inherently low-cost materials particularly attractive, especially considering much of the requirement for poisonous Hg remediation is in developing and middle-income countries. There is still great scope for variation in crosslinker structures, blending of materials, and further optimisation, and many more interesting materials are likely to be developed in the near future with yet further improved properties.

Acknowledgements

We thank Gary Bond, J. Donnelly, and T. Garcia-Sorribes for ICP analysis, S. Higgins for GPC, S. J. Green for assistance in salt templating, and M. Prestly for useful discussions. TH is a Royal Society University Research Fellow.

Notes and references

1. J. J. Griebel, R. S. Glass, K. Char and J. Pyun, *Progress in Polymer Science*, 2016, **58**, 90-125.
2. W. J. Chung, J. J. Griebel, E. T. Kim, H. Yoon, A. G. Simmonds, H. J. Ji, P. T. Dirlam, R. S. Glass, J. J. Wie, N. A. Nguyen, B. W. Guralnick, J. Park, A. Somogyi, P. Theato, M. E. Mackay, Y.-E. Sung, K. Char and J. Pyun, *Nature Chemistry*, 2013, **5**, 518-524.
3. M. Arslan, B. Kiskan, E. C. Cengiz, R. Demir-Cakan and Y. Yagci, *European Polymer Journal*, 2016, **80**, 70-77.
4. P. T. Dirlam, A. G. Simmonds, T. S. Kleine, N. A. Nguyen, L. E. Anderson, A. O. Klever, A. Florian, P. J. Costanzo, P. Theato, M. E. Mackay, R. S. Glass, K. Char and J. Pyun, *Rsc Advances*, 2015, **5**, 24718-24722.
5. J. J. Griebel, G. Li, R. S. Glass, K. Char and J. Pyun, *Journal of Polymer Science Part a-Polymer Chemistry*, 2015, **53**, 173-177.
6. A. G. Simmonds, J. J. Griebel, J. Park, K. R. Kim, W. J. Chung, V. P. Oleshko, J. Kim, E. T. Kim, R. S. Glass, C. L. Soles, Y. E. Sung, K. Char and J. Pyun, *ACS Macro Lett.*, 2014, **3**, 229-232.
7. J. J. Griebel, S. Namnabat, E. T. Kim, R. Himmelhuber, D. H. Moronta, W. J. Chung, A. G. Simmonds, K.-J. Kim, J. van der Laan, N. A. Nguyen, E. L. Dereniak, M. E. Mackay, K. Char, R. S. Glass, R. A. Norwood and J. Pyun, *Advanced Materials*, 2014, **26**, 3014-3018.
8. M. P. Crockett, A. M. Evans, M. J. H. Worthington, I. S. Albuquerque, A. D. Slattery, C. T. Gibson, J. A. Campbell, D. A. Lewis, G. J. L. Bernardes and J. M. Chalker, *Angewandte Chemie International Edition*, 2016, **55**, 1714-1718.
9. T. Hasell, D. J. Parker, H. A. Jones, T. McAllister and S. M. Howdle, *Chemical Communications*, 2016, **52**, 5383-5386.
10. M. Thielke, L. Bultema, D. Brauer, B. Richter, M. Fischer and P. Theato, *Polymers*, 2016, **8**, 266.
11. L. Jarup, *Br. Med. Bull.*, 2003, **68**, 167-182.
12. W. Feng, E. Borguet and R. D. Vidic, *Carbon*, 2006, **44**, 2998-3004.
13. H. C. Hsi, M. J. Rood, M. Rostam-Abadi, S. G. Chen and R. Chang, *Journal of Environmental Engineering-Asce*, 2002, **128**, 1080-1089.
14. W. C. Oliver and G. M. Pharr, *Journal of Materials Research*, 1992, **7**, 1564-1583.

15. P. H. Mott, J. R. Dorgan and C. M. Roland, *Journal of Sound and Vibration*, 2008, **312**, 572-575.
16. L. Blight, B. R. Currell, B. J. Nash, R. A. M. Scott and C. Stillo, in *New Uses of Sulfur—II*, AMERICAN CHEMICAL SOCIETY, 1978, vol. 165, ch. 2, pp. 13-30.
17. B. K. Bordoloi and E. M. Pearce, in *New Uses of Sulfur—II*, AMERICAN CHEMICAL SOCIETY, 1978, vol. 165, ch. 3, pp. 31-53.
18. Z. Cai, B. X. Shen, W. L. Liu, Z. Xin and H. Ling, *Energy Fuels*, 2009, **23**, 4077-4081.
19. T. A. Davidson and K. B. Wagener, *Journal of Molecular Catalysis A: Chemical*, 1998, **133**, 67-74.
20. A. E. Goetz and A. J. Boydston, *Journal of the American Chemical Society*, 2015, **137**, 7572-7575.
21. Y. S. Yang, E. Lafontaine and B. Mortaigne, *Journal of Applied Polymer Science*, 1996, **60**, 2419-2435.
22. J. W. Nicholson, in *The Chemistry of Polymers (3)*, The Royal Society of Chemistry, 2006, DOI: 10.1039/9781847552655-00023, pp. 23-39.
23. H. X. Weng, C. Scarlata and H. D. Roth, *Journal of the American Chemical Society*, 1996, **118**, 10947-10953.
24. J. Raynaud, J. Y. Wu and T. Ritter, *Angewandte Chemie-International Edition*, 2012, **51**, 11805-11808.
25. K. Satoh, *Polymer Journal*, 2015, **47**, 527-536.

